Available online at www.sciencedirect.com
SCIENCE DIRECT®

Journal of the European Ceramic Society 23 (2003) 2729–2735

www.elsevier.com/locate/jeurceramsoc

The α-alumina(0001)surface: relaxations and dynamics from shell model and density functional theory

A. Marmier, A. Lozovoi, M.W. Finnis*

Atomistic Simulation Group, School of Mathematics and Physics, Queen's University Belfast, Belfast BT7 1NN, UK

Abstract

We have investigated the dynamics and harmonic free energy of the (0001) surface of α-Al_2O_3 with both semi-empirical and ab initio techniques. The shell models provide a convenient way to to simulate the more expensive ab initio methods and to check some of their technical limitations, in particular the quality of the vibrational Brillouin zone sampling and the harmonic approximation. We have used the supercell approach to compute the frequencies of normal modes at special k-points, which allows the free energy to be calculated at different temperatures. From the corresponding phonon eigenvectors we evaluate the mean square displacements of Al and O ions. The surface phonons are particularly sensitive to the modelling technique. The ab initio surface modes are more localized and of higher amplitude, but they are not anharmonic enough to account for the discrepancy observed between the measured and calculated inward relaxation of the surface aluminium atoms.

Keywords: Interfaces; Lattice

1. Introduction

α-Alumina is arguably the simplest aluminium oxide, also the most stable thermodynamically, and a much studied model system for understanding metal oxides generally. Many technological applications (corrosion and wear protection, thin film substrates, catalyst supports) are also based on alumina surfaces and interfaces.

One of the mysteries of the surface science of alumina concerns the nature of the simplest surface, i.e. α-Al_2O_3 (0001). Experiments and calculations differ noticeably not only in the amount of relaxation of the surface, but also (albeit to a lesser extent) in the composition of the surface (Al, O, a mixture ?). Ion-scattering Refs.[1,2] and X-ray[2,3] experiments conclude that the surface is Al terminated although Refs.[1] and[3] only considered purely Al or O terminated surfaces. One of the tensor-LEED[4] analyses concluded that a 2:1 mix of Al and O terminated terraces was the best model to the data. However a more recent tensor-LEED[5,6] analysis strongly favoured the Al termination. The same conclusion is reached by the most recent ion-scattering[2] experiment, whose authors also considered mixtures of terminations as candidates. The theoretical conclusions are more consistent:all studies, whether semi-empirical[7–9] or using different flavours of ab initio, Hartree-Fock (HF)[10] or based on density functional theory (DFT),[11–15] identify the Al terminated surface as the most stable in ambient conditions. Note that more recent DFT work includes the effect of environment on the surface free energy in a very simple way, namely by taking into account the effect of a partial pressure of water,[11] hydrogen[13] or oxygen.[14] In all cases, an Al terminated surface is the most stable at oxygen partial pressures ranging from above one atmosphere down to almost the dissociation pressure of the oxide.

While there seems to be fairly good agreement that the surface is stoichiometric and Al-terminated (a relaxed bulk termination), the way the surface relaxes is not resolved yet. Experiments indicate an inward relaxation of 50–60% for the outermost Al layer, while theoretical studies suggest something nearer 70–80%. Discrepancies of this magnitude, amounting to 0.2–0.3 Å, must be regarded as a serious test for theory and experiments. Calculations which included a monolayer of hydrogen[13] improved the situation somewhat, reducing the relaxation to 69%, but this is still rather more than experimental values, and furthermore in the most recent LEED study,[6] the authors suggest that their specimen preparation should have eliminated so much hydrogen.

* Corresponding author. Tel.: +44-2890-335330; fax: +44-2890-241958.
E-mail address: m.finnis@qub.ac.uk (M.W. Finnis).

0955-2219/03/$ - see front matter © 2003 Elsevier Ltd. All rights reserved.
doi:10.1016/S0955-2219(03)00283-8

Alternatively, the discrepancy between zero-temperature calculations and room-temperature experiments could be explained if there were large ampliude, anharmonic, surface vibration modes. This has already been proposed for the (001)surfaces of TiO_2,[16] and is the explanation favoured by the authors of Ref.[6] We consider this hypothesis in our present paper. Some previous theoretical studies have been made of the dynamics of α-Al_2O_3 (0001),[8,9] but the authors did not publish details of the surface modes, and the calculations so far are only based on semi-empirical models.

The goal of this work is to study the surface dynamics of α-Al_2O_3 in suffcient detail to decide whether or not a localised soft surface mode could be responsible for the reduced relaxation as measured experimentally. Also, using the same theoretical machinery, we have obtained the vibrational contribution to the free energy (at least within the harmonic or quasiharmonic approximations), and estimate the surface free energy at non zero temperature. Our favoured approach for total energy and force-constant calculations is Plane Wave Density Functional Theory (PW-DFT), but we also use two semi-empirical shell models, as explained later.

2. Methods

We have used both first principles (ab initio) methods and classical shell models for calculating energies and forces. Ab initio PW-DFT calculations are a fairly reliable way to obtain surface properties, without relying on empirically derived parameters. Semiempirical potentials such as the shell model are very much faster to apply, and the results are easy to interpret physically. However, it is not clear how reliably they can be transfered from bulk to surface environments.

Our purpose in applying shell models here is twofold. On the one hand we can study how closely they mimic ab initio calculations, particularly regarding the surface dynamics, and on the other hand we can use them to check the convergence of certain quantities more thoroughly than would be possible with the ab initio method. These include the surface properties as a function of slab thickness and the phonon free energy as a function of k-space sampling.

We use two parameterizations of the shell model. Whereas these models are known to stabilize the bixbyite structure instead of the corundum structure for alumina, which they predict is only metastable, nevertheless their description of the relaxed structure of the (0001)surface is very comparable to the ab initio results. The parameters of these models and a more detailed discussion of their description of the (0001)surface can be found in Ref.[17] We have used the GULP code[18] for all the shell model calculations.

2.1. Slab thickness

Periodic boundary conditions are imposed in all three directions, so that a slab consisting of several atomic layers is constructed and separated from its periodic images by a layer of vacuum. To minimize slab–slab interactions, the slab and the vacuum layer have to be thick enough, which increases the computational cost. We find that a slab containing 6 stoichiometric layers (a stoichiometric layer comprises a plane of 3n oxygen atoms with a plane of n Al atoms on each side of it) is suffcient for the surface free energy to be within 0.4% of its value for 12 such layers. The surface energy for a system in which the vacuum is 6 such layers thick is within 0.1% of its value with the vacuum three times as thick.

2.2. Brillouin zone sampling

We use a periodic supercell approach to compute the dynamical matrix, so the phonon frequencies are only accessible at the Γ point of the supercell. These frequencies map onto points and directions of high symmetry for the primitive cell. For example, along $<0001>$, by trebling the length of the supercell we obtain eigenvalues and eigenvectors of the dynamical matrix corresponding to points at 1/3 and 2/3 of the way from Γ to the primitive Brillouin zone boundary at Z (see Fig. 1). This sampling has been used to approximate the integrals over the Brillouin zone that we require for estimating the harmonic free energy and atomic mean squared displacements (MSD). Here again, semi-empirical calculations allow a thorough check of the sampling of the vibrational Brillouin zone, via a Monkhorst-Pack scheme, which we have carried out up to $12\times12\times1$ k-points. We find that even just a two k-point sampling of the vibrational Brillouin zone in the slab geometry gives well converged results for the free energy and MSD of a surface.

2.3. Harmonic vs quasiharmonic

In the harmonic and quasiharmonic approximations the Helmholtz free energy at a temperature T is given by

$$F(V,T) = E(V) + \sum_{\mathrm{q},j} f_j(\mathrm{q}) \tag{1}$$

in which the contribution of the jth mode at wavevector $\mathbf{q}$ is

$$f_j(\mathbf{q}) = \frac{1}{2}h\nu_j(\mathbf{q}) + kT\ln\left[1\text{-}\exp\left(\text{-}h\nu_j(\mathbf{q})/kT\right)\right] \tag{2}$$

$E(V)$ is the potential energy of the static lattice at a volume V. The jth normal mode has frequency υ_j. Anharmonic effects are included through the explicit volume dependence of the potential energy. As noted

previously,[17] the dependance of the surface free energy on the temperature can vary strongly with the type of lattice dynamic approximation used (harmonic or quasiharmonic). We have implemented a simplified form of quasiharmonic approximation by taking into account only the homogeneous thermal expansion, obtained by minimizing F with respect to V. The free energies calculated with shell models (see also Fig. 5) show that the increase of the surface area can be at least as important as the effect due to the temperature decrease in the free energy difference.

2.4. DFT parameters

The electronic structures, total energies and harmonic frequencies were calculated with the free energy plane waves pseudopotential method in which the finite temperature density matrix is diagonalized from a Trotter factorization, as implemented in the FEMD code.[19] The conventional local density approximation is used, as in Ref.[12] The pseudopotentials are in the Kleinman-Bylander form. A PW cutoff 80 Ry was used in all calculations. The number of electronic k-points for all but 10 atom cells was chosen to correspond to 4 k-points for the 30 atom cell. The atomic positions are relaxed by steepest-descents following the Hellmann-Feynman forces.

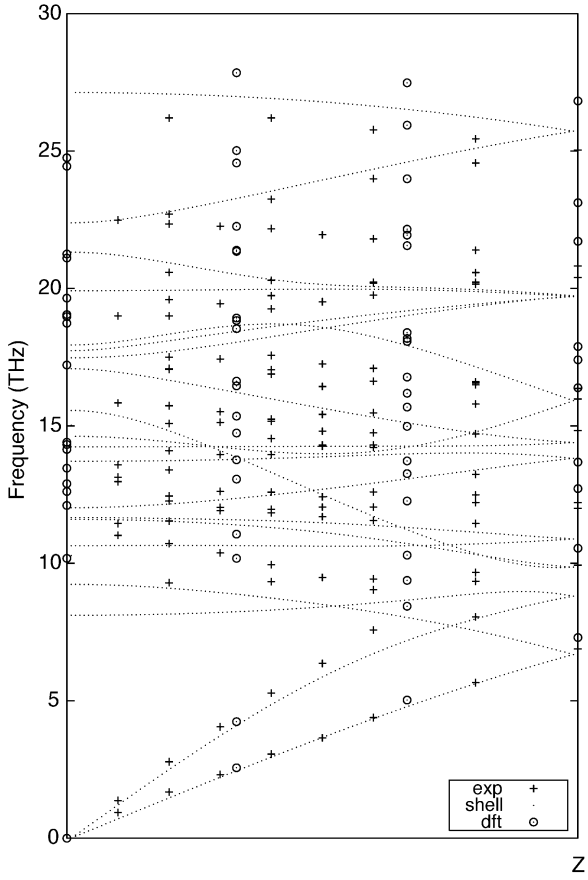

Fig. 1. Bulk α-Al_2O_3 dispersion curves along the Γ–Z direction.The crosses represent the neutron scattering results of Ref.[21], the dots the shell model 1 frequencies and the circles the DFT frequencies.

3. Results of bulk calculations

α-Alumina has the corundum structure, a rhombohedral space group $R\bar{3}C$, with two formula units per primitive cell. The crystal can also be represented as a hexagonal structure with 6 formula units per unit cell, which is useful for studying its (0001) surface. It can also be viewed as a stacking of alternating O and Al planes along the (0001) direction, according to the sequence AlO_3Al–AlO_3Al, where the oxygens in each group of three are coplanar. We used the following experimental[20] lattice parameters as a first guess for our energy minimization: $a=0.5128$ nm $\alpha=55.28$ (corresponding in the hexagonal structure to $a=b=0.4759$ nm and $c=1.299$ nm).

3.1. Structure

In the static limit, (at 0 K), the DFT corundum structure has hexagonal lattice constants of 0.459 and 1.256 nm. The contraction of 3% with respect to the experimental values is typical of LDA; the shell model potentials perform much better as they are fitted to the experimental parameters (0.4789,1.2537 and 0.4838, 1.2761 respectively for the two parameterisations).

It is relatively easy to to obtain the quasiharmonic free energy using the shell models, whereby the free energy is minimised at constant pressure for any given temperature using the GULP code.[18] The calculated expansion coefficients are 4.9 and 4.7 10^{-6} K^{-1} at 300 K.

The above procedure is not yet automated for DFT calculations; one has to calculate the free energy for different temperatures and for a range of lattice constants, and then determine for each temperature the lattice constant at which the free energy is minimum. The corresponding expansion coefficient is 2.9 10^{-6} K^{-1} at 300 K and 4.7 10^{-6} K^{-1} at 600 K, comparable, if somehow smaller than the experimental value (in the range 5.9–6.9 10^{-6} K^{-1}). Note that a more accurate calculation would involve in addition the independent relaxation of the further two internal degrees of freedom that characterize the corundum structure, besides the two cell parameters, requiring a quasiharmonic phonon calculation and free energy evaluation at each set of parameters.

3.2. Dynamics

The bulk dispersion curves are known experimentally[21] and have been calculated by DFT[22] using linear response theory. We show the dispersion curves along

the Γ-Z direction in Fig. 1. There are 20 branches, corresponding to the 10 atoms in the primitive unit cell, with longitudinal and degenerate transverse modes. Note that the frequencies of those modes that polarize the cell are not accurately accessible within the supercell scheme, since periodic boundary conditions omit the depolarizing field that splits LO and TO modes.

A second important feature is the systematic overestimation of the frequencies by the DFT. This is not uncommon (see for instance Ref.[23]) and is associated with the underestimation of the lattice constant compared to its experimental value. In retrospect however, since the surface energy calculated with the pseudopotential used here is also higher than that of other DFT calculations, we believe we could have made use of a more accurate pseudopotential.

Nevertheless, both shell model and DFT capture well the main features of the dispersion curves.

4. Surface

4.1. Structure and relaxations

The relaxation of the surface layers is very large by comparison with other materials.

The relaxations (including the results of previous work for comparison) are summarized in Table 1. It shows that a broad range of relaxations is spanned by previous calculations. With the exception of Ref.[4], all results are at least in the same direction. The distance between the outermost Al atoms (labelled Al1) and the first O plane (labeled O1)is greatly reduced (with respect to the bulk value of 79 pm), by around 50% according to most experiments, and up to 85% for DFT calculations. The magnitude of the relaxation between O1 and the second Al plane (labelled Al2) is much smaller and in all but one case positive. There is less experimental data for the deeper layers.

Table 1
Relaxations of Al terminated surfaces (percent of the relevant bulk spacing)

Method	Al1O1	O1Al2	Al2Al3	Al3O2	O2Al4
X-ray[3]	−51	−16	−29	20	–
TOF-SARS[1]	−63	–	–	–	–
LEED[4]	30	6	−55	–	–
Tensor LEED[5]	−50.0	6.3	–	–	–
HF[10]	−78.8	−3.7	−43.6	−7.9	–
LDA[11]	−85	3	−45	20	–
GGA[13]	−86	6	−49	22	6
GGA (with H)[13]	−69	–	–	–	–
GGA[12]	−69.6	10.4	−34.3	18.5	3.4
Shell,MD[9]	−58	4	−42	24–	–
Shell1 (300 K) this work	−56.9	6.9	−44.2	23.7	6.5
Shell2 (300 K) this work	−73.9	12.0	−41.6	26.6	11.5
LDA, this work	−81.8	3.6	−44.2	18.5	4.5

The first shell model relaxations give the best agreement with recent experimental results, better than either the second shell model or ab initio results. However, it would be premature to conclude that this model is more realistic than ab initio calculations, although in one respect it probably is, namely the modelling of long-range Van der Waals interactions, which DFT omits.

4.2. Dynamics

4.2.1. Surface modes

The components of the eigenvectors of the dynamical matrix are the displacements associated with each phonon. From these it possible to identify the surface modes, i.e. those where the displacements of the atoms decay to zero into the bulk.

The mode which exhibits the highest amplitude at the surface is illustrated for shell model 1 and DFT calculations in Fig. 2.

For the DFT calculation, the mode is rather more localised than for the shell model. This is especially evident for the outer Aluminium plane (Al1). As the slab has two surfaces, these localized modes appear in nearly degenerate pairs, the two surface displacements being either in-phase or out of phase. The out of phase mode polarizes the slab, so its frequency is spuriously lowered, due to the error described previously, thus we can be more confident of the in-phase frequencies and eigenvectors.

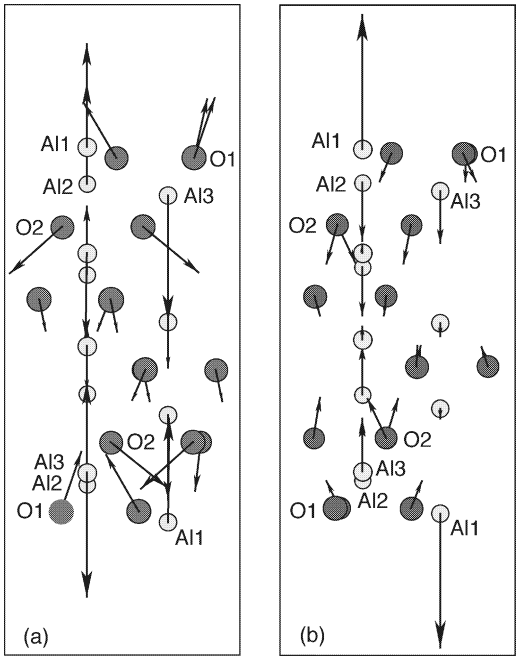

Fig. 2. Phonon mode with the most pronounced surface localisation from (a) shell model 1, and (b) DFT.

4.2.2. Mean squared displacements

We also analyse the dynamics of the slab in terms of mean–square displacements (MSD) and root–mean–square displacements (RMSD), calculated from the eigenvectors of the dynamical matrix.[24] At 350K (a temperature chosen for direct comparison with Refs.[5] and [6] we find that the RMSD is 8.9 pm for the Al atoms (10.2 and 9.9 pm for the shell models). Bearing in mind that for a simple harmonic oscillator the RMSD is related to its amplitude by a factor $1/\sqrt{2}$, these values (corresponding to amplitudes of 12.6, 14.4 and 14.0 pm respectively) compare favourably with the 12 pm estimated from Refs.[5] and [6] (see later).

We plot the MSDs of the atoms as a function of their depth in the slab for a temperatures of 300 K in Fig. 3. We have separated the two type of atoms and the perpendicular and parallel to the surface contributions to the MSD. Significant differences appear in the bulk values, which are roughly twice as large for the shell models as for DFT. There are also notable differences in the relative parallel/perpendicular contributions, and in the relative amplitude of the MSD of the surface Al atom Al1. For Al1, the RMSD perpendicular to the surface at 300 K is 88% more than in the bulk, to be compared with the ratios 32 and 48% for the two shell models. Our DFT calculations overestimate frequencies by roughly 10%, and hence should underestimate the MSDs, since the amplitudes of modes vary as the inverse square of their frequency. However, the relative results should be more reliable. A comparable source of error in this case is the two k-point approximation, as checked by fully converging the shell model results with k-points. In summary, there is a significant difference between the shell model and DFT.

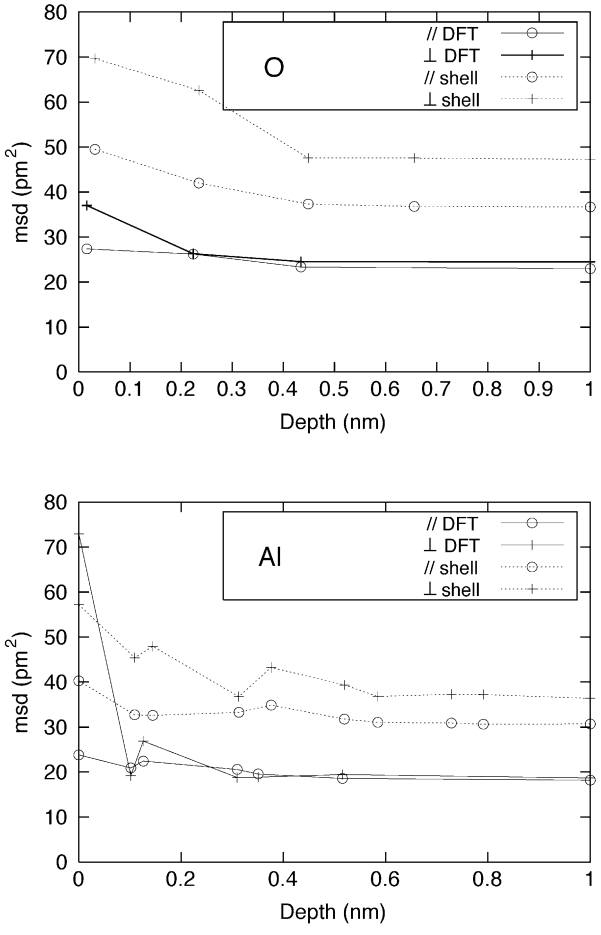

Fig. 3. Mean square displacements at 300 K. The continuous curves are the DFT values, the dashed ones are obtained with shell model 1.

The predicted large amplitude of the surface vibrations is in agreement with the results of the recent tensor LEED analysis.[5,6] In that paper, it is argued, in order to best model the experimental data, a 'split Al atom' has to be used, meaning that a mixture of two domains was used to the date, with independent variation of the atomic positions in each domain. This is simply a device to capture the range of vibrational excursions, which is represented by the difference in the position of the Al atoms in the two domains. The experimental difference in positions is about 24 pm, and is interpreted as corresponding to a large amplitude of vibration of about 12 pm.

4.2.3. Anharmonicity

At this point, it remains to be checked whether the localised modes are anharmonic enough to account for the discrepancy of about 0.02 nm in the surface relaxation. Recall that the phonon modes calculated from shell models are not so localised and the amplitude of the outermost Al atom is 'only' at most 50% more than in the bulk. This suggests that the DFT mode is a better candidate for our purpose.

We have displaced the atoms along the eigenvector of our most localised phonon mode and calculated the corresponding energy of its potential well. Fig. 4 shows the energy variation of the mode shown in Fig. 2b as a function of the displacement of the outermost Al atom. A negative value corresponds to a displacement into the surface. This procedure shows not only that the mode has too little anharmonicity to shift the mean position significantly, but also that the small effect of such anharmonicity is in the wrong direction! The equilibrium position of the outermost Al atom would be shifted in the direction of the surface (by very little), which would make the Al1–O1 distance even smaller. That is the opposite of what is required to improve agreement with experiment.

4.2.4. Surface free energy

To the best of our knowledge, there is only one previous calculation of the α-Al_2O_3 (0001)surface free energy γ_s.[8] Using semi empirical potentials, Simms showed that γ_s depends significantly on the potential used, ranging from 1.6 to 3.2 J m^{-2} at 0 K. On the other hand, the decrease of γ_s with temperature shows less of a difference between the potentials, its total variation

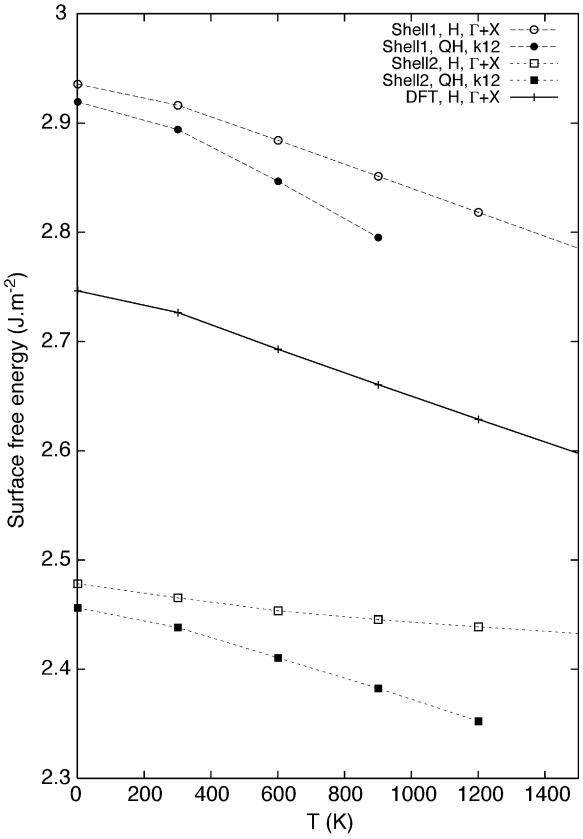

Fig. 4. Potential energy well for the high amplitude surface mode illustrated in Fig. 2b.

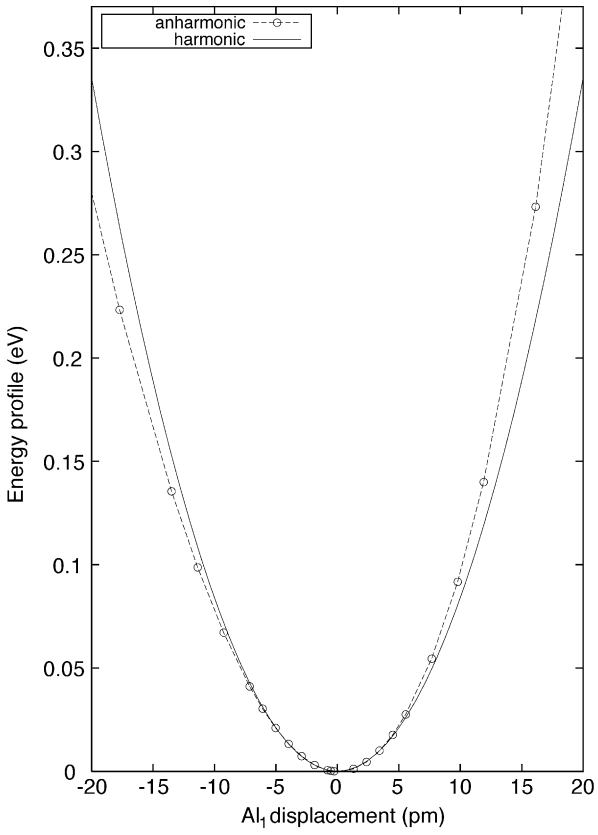

Fig. 5. Surface free energy as a function of temperature.

Table 2
Surface energy and free energy)

Method	Surface energy (J m^{-2})
Experiment[25]	2.60
LDA[26]	1.76
GGA[12]	1.95
GGA[13]	2.13
LDA[11]	1.98
GGA (LAPW)[15]	2.15
LDA (LAPW)[27]	2.59
Shell, MD (300 K)[9]	3.20
Shell1, QA (300 K)	2.89
Shell2, QA (300 K)	2.44
LDA (static limit) this work	2.64

with temperature being around −0.18 J m^{-2} over the range 0–1500 K. Calculated values of the surface energy (without the vibrational contribution) are more common. There is one experimental value, from calorimetric measurement,[25] which is is 2.6 J m^{-2}. Most theoretical values lie between 2.0 and 3.0 J m^{-2} (see Table 2).

In the static limit, we obtain a value for the surface energy of 2.63 J m^{-2}. Including zero point energy at 0 K, we get 2.750 and 2.746 J m^{-2} for sampling with one and two k-points respectively. As mentioned above, our value is rather high compared to other DFT calculations, which is probably a fault of the pseudopotential we have used.

We plot γ_s as a function of temperature in Fig. 5, as calculated with the shell models and the DFT. The solid curves represent the full quasi-harmonic results, while the broken curves and the DFT results refer to the harmonic approximation with just 2 k-points. The comparison between these sets of curves for the two shell models and the ab initio surface free energy, which they bracket, shows that we can expect the quasiharmonic value of γ_s to decrease more steeply with temperature. This is mostly a consequence of the fact that the harmonic approximation does not take into account the increase in surface area due to thermal expansion. The two k-point sampling appears to be a good approximation (see also Ref.[17]). Fully quasiharmonic DFT calculations are very time consuming and are still in progress.

5. Conclusions

We have calculated structural and dynamical properties for the stoichiometric, Al terminated (0001)surface of α-Al_2O_3 using an ab initio DFT description in the harmonic approximation, and two shell models in the quasi-harmonic approximation.

As with all preceding ab initio simulations of this surface, we find unusually large relaxations. These would be in satisfactory agreement with experimental findings, were it not for the size of the relaxation of the surface Al, consistently predicted by DFT (and the most recent Hartree-Fock calculations) to be around 80%, whereas recent experiments suggest only 50% (a difference in absolute spacing of 24 pm). Our present study has focussed on examining the possibility that this discrepancy is due to large amplitude, anharmonic, surface vibrations, not considered in the 0 K calculations.

By diagonalizing the dynamical matrix for a supercell containing a slab, we find a mode localised on the two outer stoichiometric planes. It is characterised by large excursions of the surface Al, with a root mean square amplitude of about 9 pm at room temperature. With the shell models it is a little more (10 pm). Our DFT model may have somewhat underestimated this amplitude, since it overestimates the phonon frequencies by several percent. However, relative to the bulk amplitudes, this mode is more localised in the DFT case and therefore has a *higher* amplitude on the surface Al than the corresponding mode with the shell models. Nevertheless, and rather surprisingly, the localised mode is only weakly anharmonic. Hence our results cannot support the hypothesis of Ref.,[5] that anharmonicity can explain the discrepancy in the measured and predicted mean surface relaxations. This conclusion holds equally for the shell models and our density functional model. We should note that the study of the anharmonicity of the normal modes has only been performed at the γ and X points of the surface Brillouin zone; it seems unlikely, but we cannot rule out the possibility, that modes with different wave vectors could be more anharmonic. However, also surprisingly, the anharmonicity that we have found is in the sense of bringing the surface Al even closer to the bulk, which is opposite to the discrepancy we are seeking to resolve.

Whether thermal effects alone or effects of the chemical environment of the surface can account for the relaxation discrepancy is not finally resolved, but both hypothesis now seem to us somewhat less likely than the intrinsic inaccuracy of the current density functional approaches (using LDA or GGA) for this problem.

References

1. Ahn, J. and Rabelais, J. W., *Surface Science*, 1997, **388**, 121.
2. Suzuki, T., Hishita, S., Oyoshi, K. and Souda, R., *Surface Science*, 1999, **437**, 289.
3. Guénard, P., Renaud, G., Barbier, A. and GautierSoyer, M., *Surface Review and Letters*, 1998, **5**, 321.
4. Toofan, J. and Watson, P. R., *Surface Science*, 1998, **401**, 162.
5. Walters, C. F., McCarthy, K. F., Soares, E. A. and VanHove, M. A., *Surface Science*, 2000, **464**, L732.
6. Soares, E. A., VanHove, M. A., Walters, C. F. and McCarthy, K. F., *Physical Review B*, 2002, **65**, 195405.
7. Mackrodt, W. C., Davey, R. J. and Davey, S. N., *Journal of Crystal Growth*, 1987, **80**, 441.
8. Simms, C.E. PhD, University of Bristol,1999.
9. Baudin, M. and Hermansson, K., *Surface Science*, 2001, **474**, 107.
10. Gomes, J. R. B., de, I., Moreira, P. R., Reinhardt, P., Wander, A., Searle, B. G., Harrison, N. M. and Illas, F., *Chemical Physics Letters*, 2001, **341**, 412.
11. DiFelice, R. and Northrup, J. E., *Physical Review B*, 1999, **60**, R16287.
12. Batyrev, I. G., Alavi, A., Finnis, M. W. and Deutsch, T., *Physical Review Letters*, 1999, **82**, 1510.
13. Wang, X-G., Chaka, A. and Scheffler, M., *Physical Review Letters*, 2000, **84**, 3650.
14. Batyrev, I. G., Alavi, A. and Finnis, M. W., *Physical Review B*, 2000, **62**, 4698.
15. Zhang, W. and Smith, J. R., *Physical Review Letters*, 2000, **85**, 3225.
16. Harrison, N. M., Wang, X. G., Muscat, J. and Scheffler, M., *Faraday Discussions*, 1999, **114**, 305.
17. Marmier, A. and Finnis, M. W., *Journal of Physics:Condensed Matter*, 2002, **14**, 7797.
18. Gale, J. D., *JCS Faraday Transactions*, 1997, **93**, 629.
19. Alavi, A., Kohanoff, J., Parrinello, M. and Frenkel, D., *Physical Review Letters*, 1994, **73**, 2599.
20. Lee, W. E. and Lagerlof, K. P. D., *Journal of Electron Microscopy Technique*, 1985, **2**, 247.
21. Schober, H., Strauch, D. and Dorner, B., *Zeitschrift für Physik B—Condensed Matter*, 1993, **92**, 273.
22. Heid, R., Strauch, D. and Bohnen, K.-P., *Physical Review B*, 2000, **61**, 8625.
23. Frank, W., Elsässer, C. and Fähnle, M., *Physical Review Letters*, 1995, **74**, 1791.
24. Maradudin, A. A., Montroll, E. W. and Weiss, G. H., *Lattice Dynamics in the Harmonic Approximation. Solid State Physics, Supplement 3*. Academic Press, New York, 1963.
25. McHale, J. M., Auroux, A., Perrota, A. J. and Navrotsky, A., *Science*, 1997, **277**, 788.
26. Manassidis, I. and Gillan, M. J., *Journal of the American Ceramics Society*, 1994, **77**, 335.
27. Zhang, W. and Smith, J. R., *Physical Review B*, 2000, **61**, 16883.